

1 *Dear Editor,*
2 *We would like to thank you for your encouraging comments. We are sure that the manuscript will*
3 *greatly benefit from your suggestions. All the reviewers' suggestions and comments have been*
4 *taken into consideration, and modified version of the manuscript were already uploaded. Hereafter*
5 *the list of Your comments is reported, followed by our response. We will also provide a version of*
6 *the manuscript with the tracked revisions of Your comments, while the referees' ones are embedded*
7 *in the text.*

8

9 **Editor:** In section 4, the adopted monitoring system, the time line rationale of the Rotolon
10 monitoring system and emergency management procedures is depicted in figure 6, but without any
11 description in the text. To improve this section could be useful to move the text of lines 281-286 in
12 section 4.

13 Moreover, a better description of the functioning of the early warning system and how the GB-
14 InSAR is employed in it, is needed.

15 **Authors:** *The shift of suggested lines has been made and more information are now in the*
16 *manuscript. Moreover, the Figure 6 has been improved.*

17

18 **Editor:** Then, the name of section 4 could be changed into The GB-InSAR monitoring strategy in
19 the Rotolon early warning system.

20 **Authors:** *The title of section 4 has been changed following the suggestion.*

21

22 **Editor:** A description about how the thresholds for the 3 levels of warning (line 284) have been
23 defined and which type of actions to undertake in each level of warning will be considerably
24 improve the paper.

25 **Authors:** *We add a sentence to explain how the thresholds were defined and the action to*
26 *undertake in each level of warning.*

27

28 **Editor:** The Discussion should be improved describing the role of the GB-InSAR in the decisional
29 process of the Rotolon monitoring system and emergency management procedures. In particular,
30 how the GB-InSAR monitoring influences the decision of issuing an alert? Reading lines 288-291
31 seems the 4 monitoring alerts issued were false alerts, because "Inspections carried out by the
32 optical monitoring device and by means of field surveys from safe viewing points, assessed that
33 detected accelerations did not generate significant slope failures". Following these considerations it

seems the GB-InSAR needed to be used coupled with other monitoring strategies in order to avoid false alerts. Please discuss.

Authors: *The role of the GB-InSAR was better specified in section 4 (The GB-InSAR monitoring strategy in the Rotolon early warning system) and 6 (Discussion). With these explanations, we have also clarified the problem of “alerts” and the necessity of coupling with other instruments.*

Specific comments

Editor: Line 126. Please specify the full name for LOS. The first time you use an acronym the full name is needed.

Line 137. Please change “parallel to the line of sight (L.O.S.)”, with “parallel to LOS”. The full name of the acronym LOS has been specified in line 126.

Authors: *The necessary adjustments have been made.*

Editor: Line 282. Is Figure 5 or 6?

Authors: In this line, we are referring to figures 5 and 7. Therefore, the text is right.

Editor: Lines 288-289 outline the issuing of 4 monitoring alerts. What the authors mean for monitoring alert? Does it means the threshold exceedance of 5mm/h, i.e. alarm level? Please, explain.

Authors: *The sentence has been better specified, indicating also the alert class according to the thresholds considered*

GB-InSAR monitoring of slope deformations in a mountainous area affected by debris flow events

William Frodella¹, Teresa Salvatici¹, Veronica Pazzi¹, Stefano Morelli¹, Riccardo Fanti¹

1. Department of Earth Sciences, University of Firenze, Via La Pira 4, 50121, Florence, Italy

Correspondence to: William Frodella (william.frodella@unifi.it)

Abstract

Diffuse and severe slope instabilities affected the whole Veneto region (Northeast Italy) between October 31st and November 2nd 2010, following a period of heavy and persistent rainfall. In this context on November 4th 2010 a large detrital mass detached from the cover of the Mt. Rotolon deep seated gravitational slope deformation (DSGSD), located in the upper Agno River Valley, channelizing within the Rotolon Creek riverbed and evolving into a highly mobile debris flow. The latter phenomena damaged many hydraulic works, also threatening bridges, local roads, together with the residents of the Maltaure, Turcati and Parlati villages located along the creek banks and the Recoaro Terme town. From the beginning of the emergency phase, the Civil Protection system was activated, involving the National Civil Protection Department, Veneto Region and local administrations' personnel and technicians, as well as scientific institutions. On December 8th 2010 a local scale monitoring system, based on a ground based interferometric synthetic aperture radar (GB-InSAR), was implemented in order to evaluate the slope deformation pattern evolution in correspondence of the debris flow detachment sector, with the final aim of assessing the landslide residual risk and manage the emergency phase. This paper describes the results of a two years GB-InSAR monitoring campaign (December 2010 - December 2012), its application for monitoring, mapping, and emergency management activities, in order to provide a rapid and easy communication of the results to the involved technicians and civil protection personnel, for a better understanding of the landslide phenomena and the decision-making process in a critical landslide scenario.

1 Introduction

Deep seated gravitational slope deformations (DSGSD) are normally not considered hazardous phenomena, due to their typically very slow evolution; nevertheless, under certain conditions ground movements can accelerate evolving into faster mass movements, which may favour collateral landslide processes (Crosta, 1996; Crosta and Agliardi, 2003). Therefore, a multidisciplinary approach is fundamental in order to understand the complex nature of such phenomena, so as to assess the correct mitigation measures. In this framework advanced mapping methods, based on spaceborne, aerial and terrestrial remote sensing platforms, represent the optimal solution for landslide detection, monitoring and mapping in various physiographic and land cover conditions, particularly with large phenomena and hazardous non accessible sectors (Casagli, 2017b; Guzzetti et al., 2012). In recent decades, many advanced remote sensing technologies have gained widespread recognition as efficient remote surveying techniques for the characterization and monitoring of landslide-affected areas, in terms of resolution, accuracy, data visualization, management, and reproducibility. Among these are: digital photogrammetry (Chandler, 1999; Zhang et al., 2004), laser scanning (Abellan et al., 2006; Gigli et al., 2012, 2014c; Jaboyedoff et al., 2012; Tapete et al., 2012), Infrared Thermography (Teza et al., 2012; Gigli et al. 2014a, b; Frodella et al., 2015) and radar interferometry, both terrestrial and satellite (Luzi et al., 2004;

101 Casu et al., 2006; Bardi et al., 2014; Tofani et al., 2014; Ciampalini et al., 2016; Gullà et al., 2017; Nicodemo et al.,
 102 2016; Peduto et al., 2017a,b).

103 Ground based interferometric synthetic aperture radar (GB-InSAR) systems in particular, for their ability to measure
 104 displacements with high geometric accuracy, temporal sampling frequency, and adaptability to specific applications
 105 (Monserrat et al., 2014), represent powerful devices successfully employed in: a) engineering and geological
 106 applications for detecting structural deformation, and surface ground displacements (Tarchi et al., 1997; 2003;
 107 Antonello et al., 2004; Casagli et al., 2010; 2017a, b) for the monitoring of volcanic activity (Nolesini et al., 2013; Di
 108 Traglia et al., 2014a, b, c) for analysing the stability of historical towns built on isolated hilltops (Luzi et al., 2004;
 109 Frodella et al., 2016; Nolesini et al., 2016). Furthermore, in recent years GB-InSAR technique has developed to an
 110 extent where it can significantly contribute to the management of major technical and environmental disasters (Del
 111 Ventisette et al., 2011; Broussolle et al., 2014; Lombardi et al., 2017; Bardi et al., 2017a, b). Between October 31st 2010
 112 and November 2nd 2010 the whole Veneto region territory (north-eastern Italy; Fig. 1) was hit by heavy and persistent
 113 rainfall, that triggered widespread flooding and abundant slope failures, causing extensive damage to people (3 fatalities
 114 and about 3500 evacuated people) and structures., not to mention heavy economic losses in agricultural, livestock, and
 115 industrial activities.

116 In this context on November 4th 2010, part of detrital cover of the Rotolon DSGSD suffered the detachment of a mass
 117 approximately 320000 m³ in volume, which channelized in the Rotolon Creek bed causing a large debris flow. This
 118 phenomenon was characterized by more than three kilometres of run-out, damaging various hydraulic works (creek
 119 dams, weirs, bank protections), and threatening various structures (bridges, local roads, houses) together with those
 120 residing in the villages of Maltaure, Turcati, Parlati and the town of Recoaro Terme; Fig. 1).

121 On December 8th 2010 a GB-InSAR monitoring system was implemented in order to assess the landslide residual
 122 displacements and support the local authorities in the emergency management (Fidolini et al., 2015), calling into play
 123 both the national (DPC) and regional (DPCR) civil protection departments, in cooperation with scientific institutions
 124 (namely “competence centres”, CdCs), local administration personnel and technicians (Bertolaso et al., 2009; Pagliara
 125 et al., 2014; Ciampalini et al., 2015). Accurate geomorphological field surveys were also carried out in this phase, in
 126 order to analyse the landslide morphological features and improve the radar data interpretation (Frodella et al., 2014;
 127 2015; 2017). In addition, a 3D landslide runout numerical model was performed to identify the source and impact areas
 128 of potential debris flow events, flow velocity and deposit distribution within the Rotolon creek valley (Salvatici et al.,
 129 2017).

130 This work is focused on the results of a long-term continuous GB-InSAR monitoring campaign (December 2010 -
 131 December 2012) carried out during the post-event recovery phase, in which monitoring, mapping, and emergency
 132 management activities were implemented to assess the landslide residual risk and analyse its kinematics. In this context
 133 field activities were carried out by local Civil Protection operators and technicians for a validation of the remotely
 134 sensed data (landslide area inspections). In particular, the analysed radar data were shared with the technicians and civil
 135 protection personnel involved in order to provide a rapid and easy communication of the results, and enhance the
 136 synergy of all the subjects involved in the recovery phase.

137

138 2. Study area

139 The Rotolon DSGSD is located in the Vicentine Prealps, on the south-eastern flank of the Little Dolomites chain, in the
 140 uppermost Agno river valley (Fig. 1). The instability processes of the area, such as slope failures and debris flows
 141 induced as secondary phenomena of the DSGSD, have threatened the upper Agno valley for centuries (Frodella et al.,

2014). From a geological point of view, the landslide develops in the uppermost portion of a mainly dolomitic-limestone stratigraphic succession, sub-horizontally bedded from middle Triassic to lower Jurassic in age, belonging to the South Alpine Domain (De Zanche and Mietto, 1981).

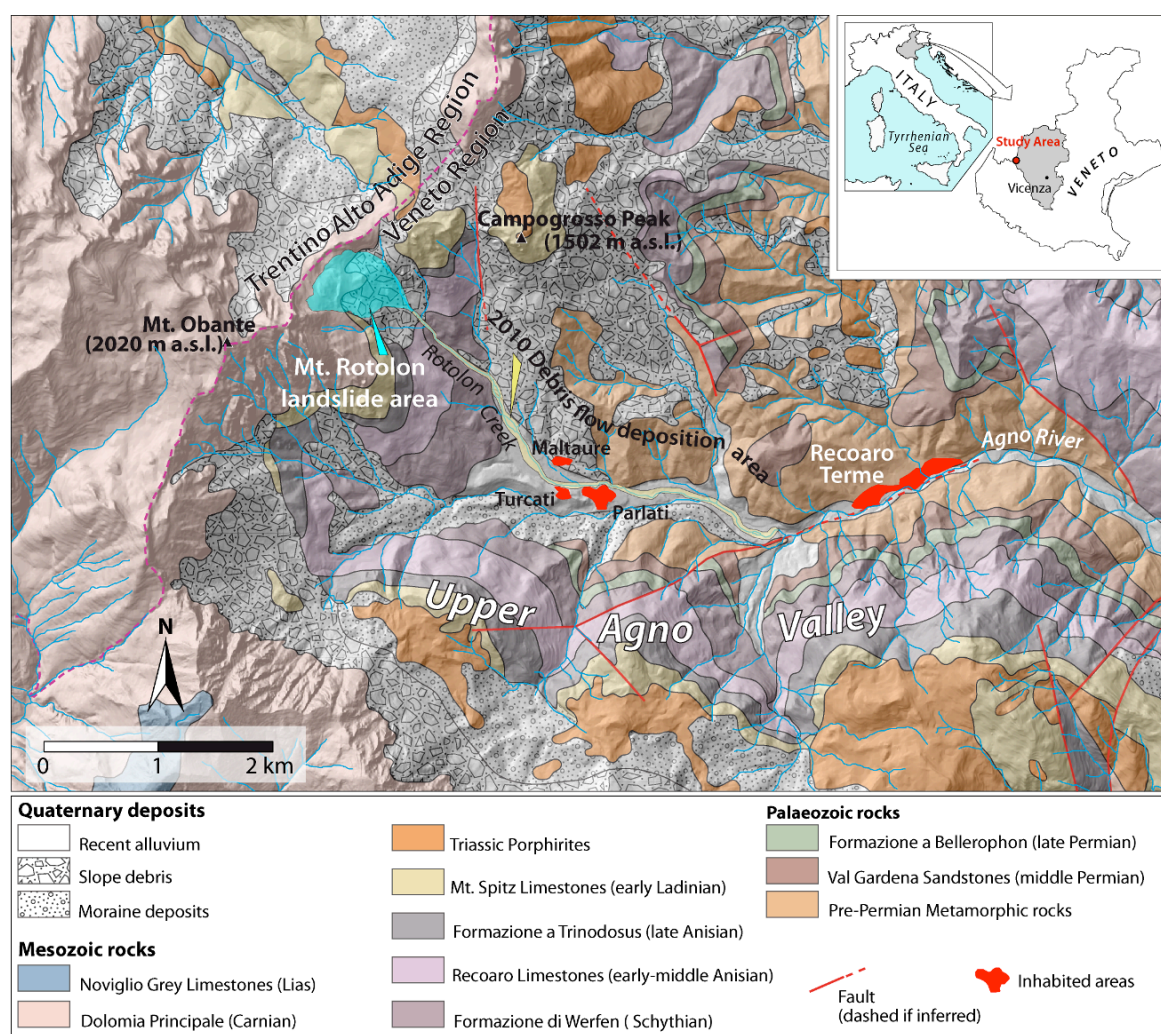


Figure 1. Geological sketch map of the Upper Agno River Valley with the location of the Rotonol landslide.

The mass movement is delimited to the NW by the ridge of the Mount Obante group and develops from about 1700 to 1100 m a.s.l., covering an area of 448000 m². The Rotonol DSGSD can be classified as a DSGSD (“sackung type”; Zischinsky, 1969), and characterized by a complex activity (Cruden and Varnes, 1996) causing a rough morphology with steep scarps, trenches, crests and counterscarps (Figs. 2 and 3).

Two distinct sectors can be identified, based on the dominant slope instability processes in act: i) an upper “detachment sector”, followed downstream by a ii) “dismantling sector” (Frodella et al., 2014). The detachment sector (with a mean slope of 30°), develops downstream from the main landslide crown (Figs. 2a and b; Fig. 3), and is dominated by extensional deformation causing the development of tensional fractures, resulting in alternate trenches and crests creating a very rough, stepped topographic surface. This area is affected by gravitational and erosional processes, as well as the rock mass detensioning and disaggregation, resulting in the accumulation of various depositional elements (colluvial fans, colluvial aprons, rock fall and rock avalanche deposits) formed by very coarse heterometric clasts, ranging from cobbles to boulders with scattered blocks (decimetric to decametric in size) in a coarse sandy matrix (Figs. 3 and 4).

161 The dismantling area (mean slope of 34°) includes sectors formed by highly weathered sub-vertical rock walls. It is
 162 dominated by surface processes (e.g., concentrated and diffuse erosion, slope-waste deposition due to gravity, detrital
 163 cover failures) that substantially cover the evidence of deeper deformations (Figs. 3 and 4). This area supplies material
 164 for debris flows, which channelize downstream within the Rotolon creek bed, representing the most critical sector for
 165 short-term hazardous phenomena.
 166



167
 168 **Figure 2.** The Mt. Rotolon DSGSD plan (a); landslide sectors (b, c) and the 2010 debris flow features (d, e).

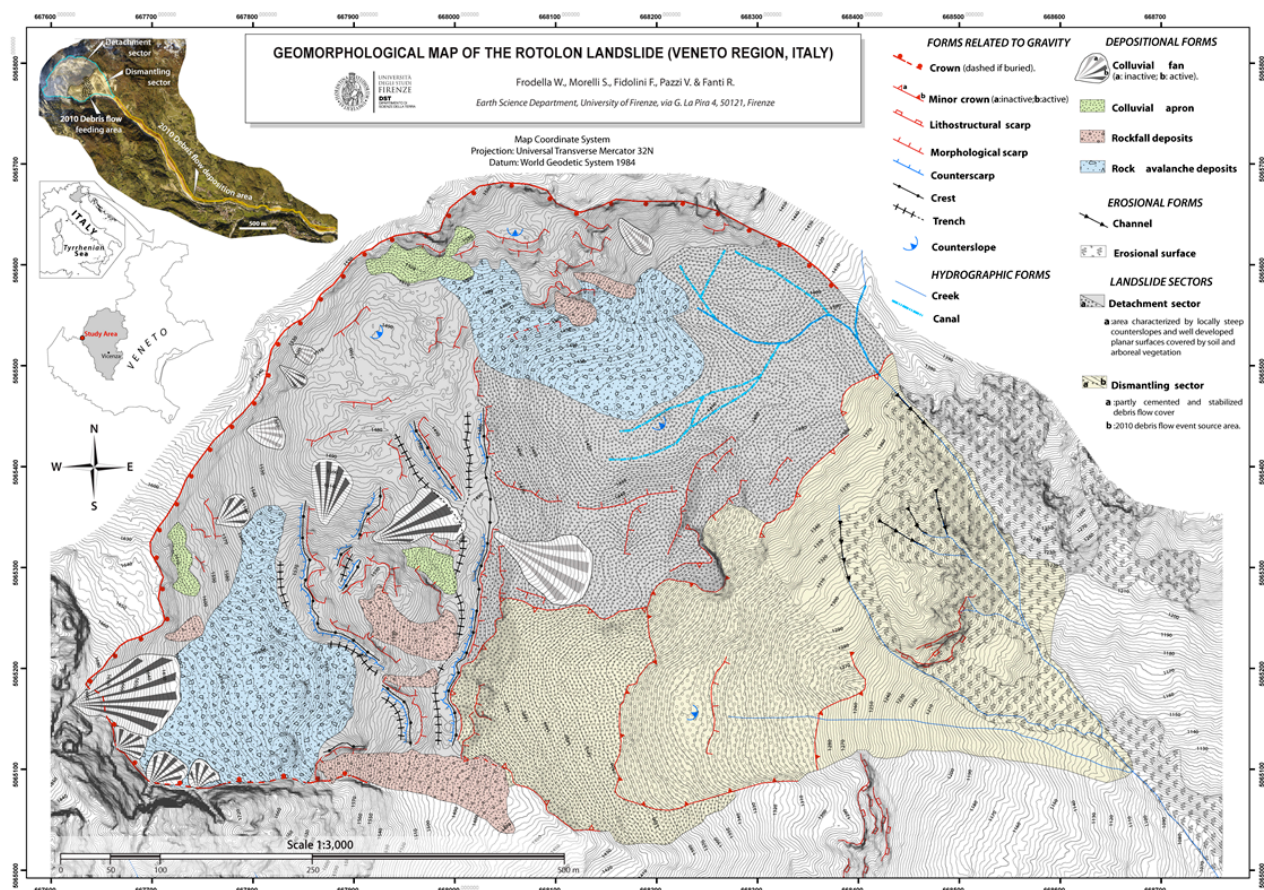


Figure 3. Geomorphological map of the Rotolon Landslide (modified after Frodella et al., 2014).

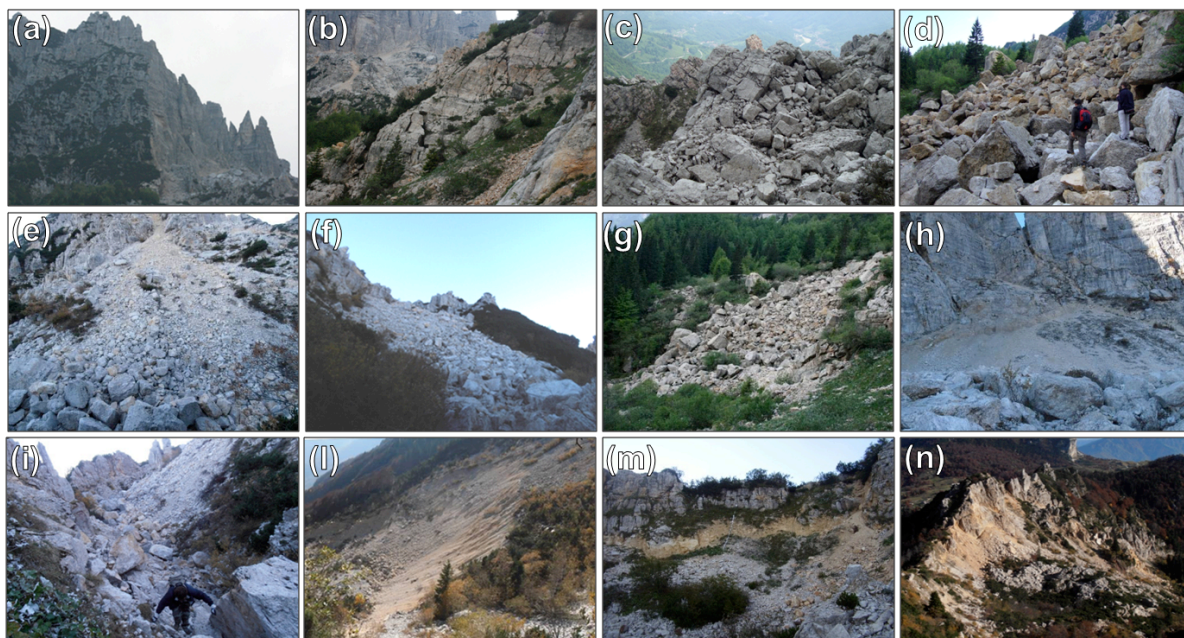


Figure 4. Geomorphic and sedimentary features of the Mt. Rotolon DSGSD detachment sector: (a) rock walls prone to rock falls; (b, c) rock mass affected by different stages of disaggregation; (d) plurimetric rock blocks within rock avalanche deposit. Main depositional elements within the landslide body: (e) colluvial fan; (f, g) channelized and diffused rock fall deposits; (h) colluvial aprons. Main landslide linear elements: (i) landslide trench; (l) 2010 debris flow detachment scarp; (m) DSGSD crown sector; (n) landslide crest.

3. The GB-InSAR technique basic theoretical principles

The GB-InSAR is a computer-controlled microwave transmitting and receiving antenna that moves along a mechanical linear rail in order to synthesize a linear aperture along the azimuth direction (Tarchi et al., 1997). The device radiates microwaves in the Ku band (12-18 GHz) and registers the backscattered signal in the acquiring time interval (less than 1 minute with the most modern systems). Each acquisition produces a complex matrix of values from which phase and amplitude information are calculated (Luzi et al., 2004; Luzi, 2010). A SAR image contains amplitude and phase information of the observed objects' backscattered echo within the investigated scenario, and it is obtained by combining the spatial resolution along the direction perpendicular to the rail (range resolution, ΔR_r) and the one parallel to the synthetic aperture (azimuth or cross-range resolution, ΔR_{az}) (Luzi, 2010). The working principle of the GB-InSAR technique is the evaluation of the phase difference, pixel by pixel, between two pairs of averaged sequential SAR complex images, which forms an interferogram (Bamler and Hartl, 1998). The latter does not contain topographic information, given the antennas fixed position during different scans (zero baseline condition). Therefore, in the elapsed time between the ~~acquisition~~acquisitions of two or more subsequent coherent SAR images, it is possible to derive from the obtained interferograms a 2D map of the displacements that occurred along the sensor LOS (Line of Sight; Tarchi et al., 1997; 2003; Pieraccini et al., 2000; 2002). The capability of InSAR to detect ground displacement depends on the persistence of phase coherence (ranging from 0 to 1) over appropriate time intervals (Luzi, 2010). Among the technique's advantages it must be noted that GB-InSAR works: a) without any physical contact with the slope, avoiding the need of accessing the area; b) in almost any light and atmospheric condition; c) continuously over a long time; d) with millimetric accuracy (the accuracy of the measured phase is usually a fraction of the operated wavelength; Luzi, 2010); e) providing extensive and detailed near real time information of the whole visible slope. This latter feature in particular gives a strong advantage with respect to traditional ground surface methods (like inclinometers, extensometers, total stations), which on the contrary provide single-point information in accessible area, and are generally not sufficient to evaluate the kinematics and potential behaviour of a complex landslide. The main drawback of the technique is the logistics of the installation platform, both because the GB-InSAR system measures only the displacement component parallel to ~~the line of sight (L.O.S.)~~LOS, and because the azimuth resolution (the ability to separate two objects perpendicular to the distance between the sensor and the target) lessens with the increase of the distance from the target (Fig. 5). Moreover, vegetated areas can be another drawback of the technique since they are commonly characterized by signal low coherence and power intensity.

4. The GB-InSAR monitoring strategy in the Rotolon early warning system~~The adopted monitoring system~~

The GB-InSAR system was installed in the Maltaure village, at an average distance of 3 km from the landslide, pointing upwards to NW (Fig. 5). The radar parameters are summarized in Fig. 5. Given the acquisition setting of the site and the civil protection needs, the radar data covers an area of 1.2 km². The logistics of the GB-InSAR system installation favoured a good spatial coverage of the data on the monitored area, especially with regards to the dismantling sector. Nevertheless, shadowing effects, due to the slope roughness, crests and counter-slope surfaces affect the detachment sectors (Figs. 5 and 7).

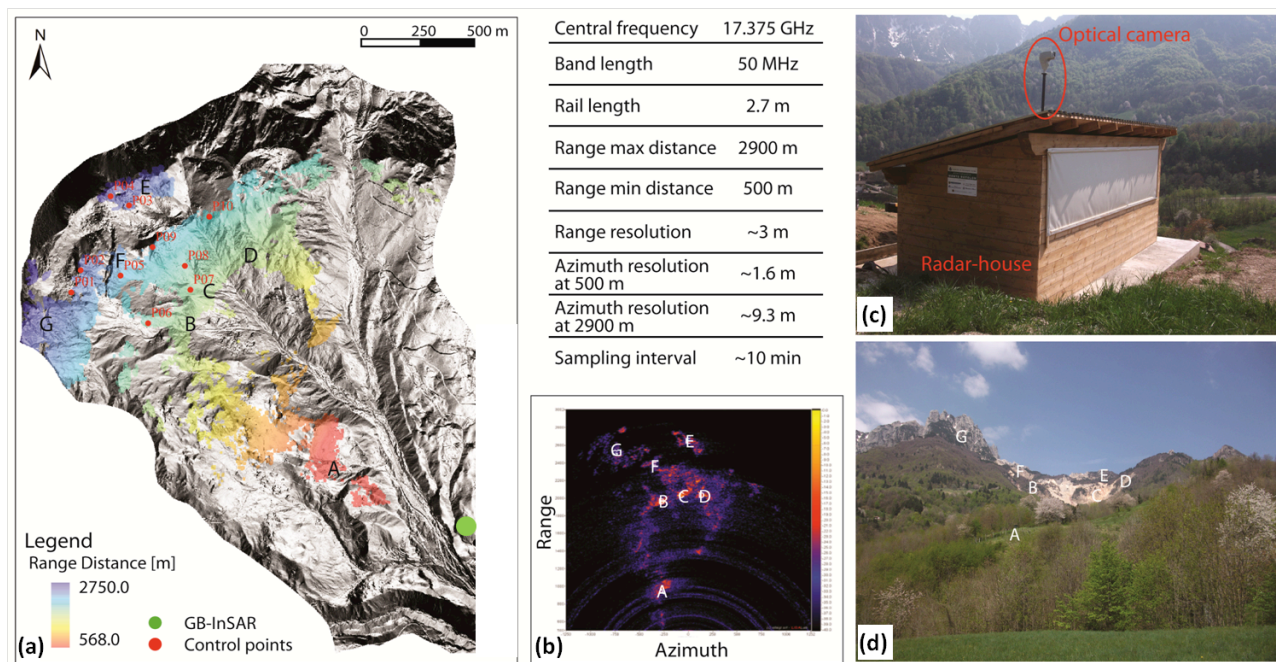


Figure 5. The adopted monitoring system: (a) Location of the GB-InSAR system and radar data coverage features (A-G=recognized landslide sectors); (b) the adopted monitoring parameters and radar power image, displaying the correspondent recognized landslide sectors; (c) the radar system hut setting; (d) picture of the monitoring optical system scenario (A-G=corresponding sectors).

The radar system acquired GB-InSAR data every 10 minutes, from which cumulated 2D displacement maps, and displacements time series of 10 measuring points (Fig. 5) were obtained. GB-InSAR data were processed using LiSALab software (Ellegi s.r.l.) and uploaded via LAN network: i) on a dedicated Web-based interface, allowing for a near real time data on-routine visualization; ii) on a remote ftp server (in ASCII format), in order to perform on demand analysis in case of critical weather events forecast by the national civil protection weather system (Fig. 6). The latter were performed integrating into a GIS environment the displacement maps and comparing them with ancillary data (rainfall, geological and geomorphological maps). In addition, a remotely adjustable robotized high resolution optical camera (Ulisse Compact model produced by Videotec S.p.A, digital zoom 10x - 36x), ~~manouverable~~ manoeuvrable via IP-Ethernet interface, was installed in correspondence with the radar system, acquiring data every 60 minutes and allowing for programmable zooms. The objective of this device was to check the hazardous and inaccessible ~~Dismantling-dismantling~~ sector of- the landslide (Figs. 5 and 6).

Based on these displacements acquisition modes, a local scale early warning system (Intrieri et al., 2012; 2013) was implemented considering three different levels of attention: ordinary, pre-alarm and alarm levels (Figure 5). In order to support the Civil Protection decision making, hourly displacement thresholds were adopted. The level change occurred if the following thresholds were surpassed: i) ordinary: <0.1 mm/h; ii) pre-alarm: 0.1 mm/h to 0.5 mm/h; iii) alarm level: >0.5 mm/h. For each threshold different actions were planned: i) regular monitoring but no additional actions; ii) on demand monitoring data and analysis, and four-hours bulletins; iii) integration with other external monitoring data and activation request of the alert system once false warnings are prevented. This last point was achievable thanks to the ability of the radar output data to be integrated and promptly analysed in a commensurable manner with records from different devices. In this specific case they were represented by traditional instruments (1 total station with a benchmarks network, 1 rain gauge and 6 extensometers; Frigerio et al., 2014) operated by the Research Institute for Geo-Hydrological Protection of the Italian National Research Council (IRPI-CNR). To define these stability thresholds,

since there was no a previous knowledge of the phenomenon behaviour, a deeper inspection of cumulated images (incremental method) and interferograms (rolling method) were carried out in the first month of activity in 7 sectors visible from the station and characterized by high reflectivity (mainly rocky and bare terrains), including the landslide area and all the surrounding slopes which were considered stable (A-G in Fig. 5). This double analysis, useful to overcome possible misinterpretations caused by noise signal, was finally refined in relation to expected dynamics of the investigated instable slope. During of all the monitoring period, communication with the deputy commissioner and cooperators was operated through the dispatch of informative bulletins every week and whenever the warning thresholds were exceeded. The time line rationale of the monitoring system and emergency management procedures is summarized in Fig. 6.

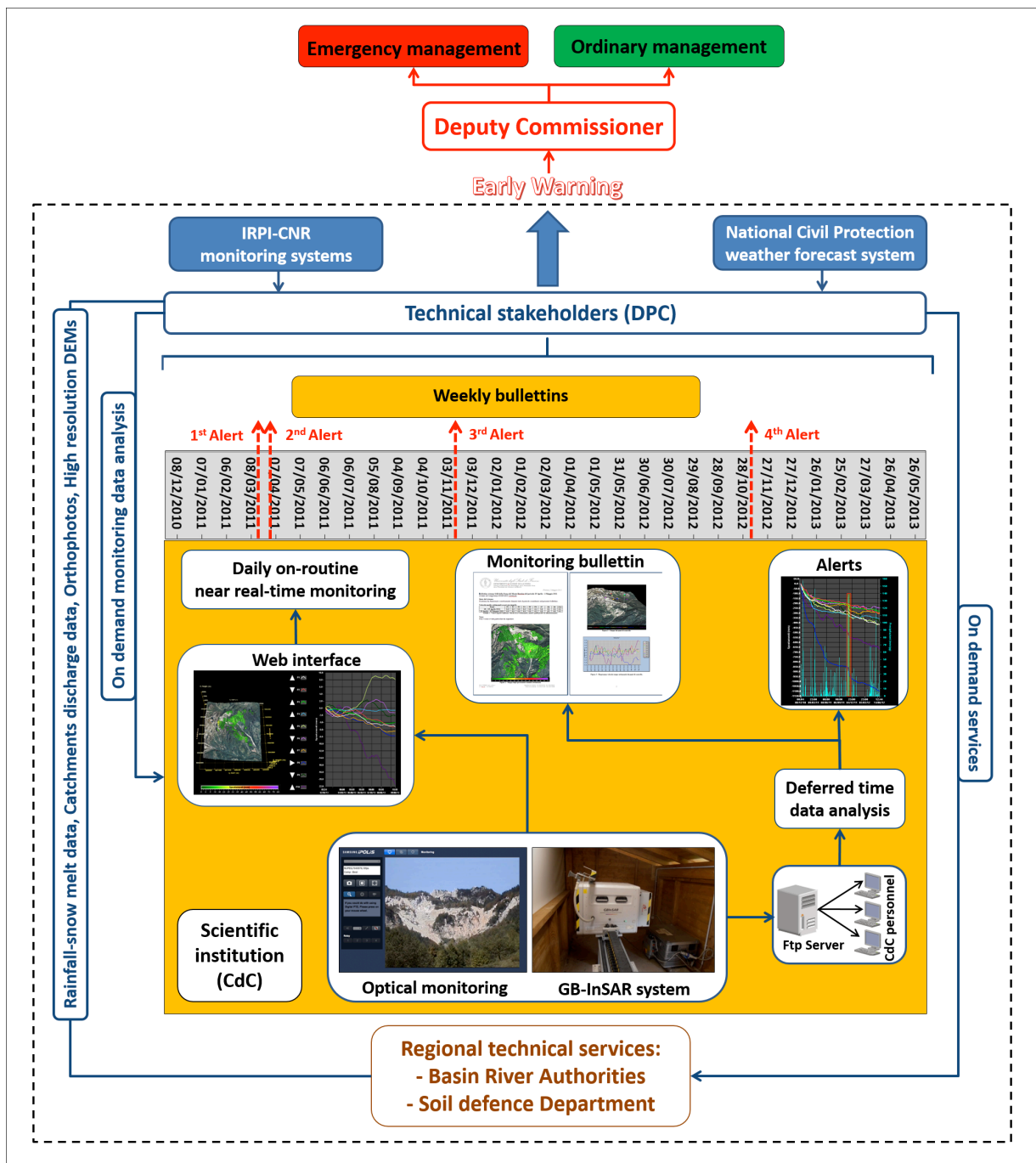


Figure 6. Time line rationale of the Roton monitoring system and emergency management procedures. The black dashed box include the early warning system.

5. GB-InSAR data analysis

The GB-InSAR incremental cumulative displacement (ICD) maps and the displacement time series of the measuring points obtained are shown in Figs. 7 and 8, respectively. By using a selected colour scale, the radar maps obtained are displayed as a function of the displacement measured in the period spanning from December 8th 2010 up to the beginning of each month of the monitoring campaign, (the negative displacement values indicate movements approaching the sensor; Fig. 7). In order to evaluate the deformation rates and provide easily interpretable data, a traffic light-type colour scale was applied in all the displacement maps.

GB-InSAR measuring points (corresponding to a 5 x 5 pixel size area) were selected in correspondence with sectors where the radar signal is characterized by high stability, in order to monitor the landslide kinematics and characterize the various landslide physiographic features (Fig. 7). Furthermore, with the aim of performing a temporally detailed displacement analysis and detecting the spatial pattern of residual landslide deformation, monthly cumulated displacement (MCD) maps were also selected and analysed from the collected GB-InSAR dataset (Fig. 9).

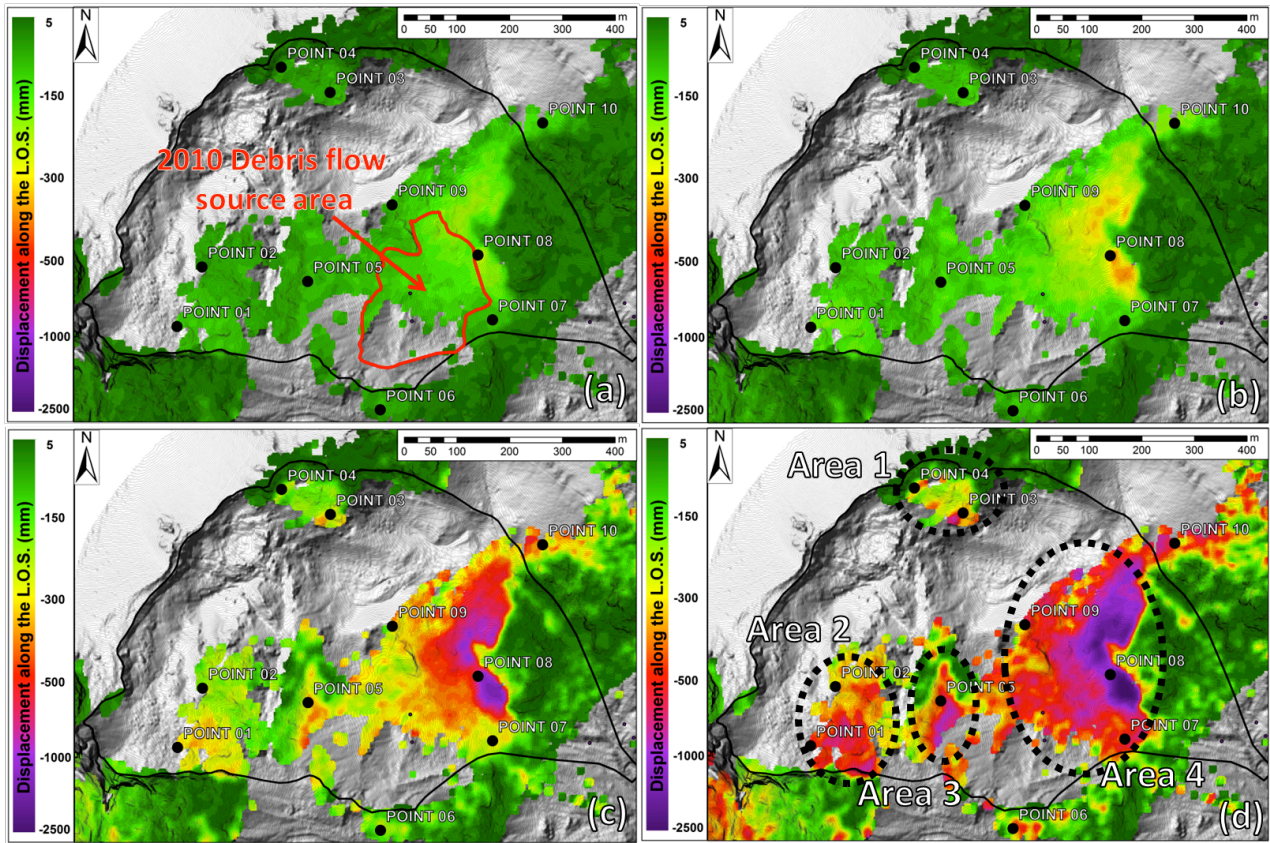
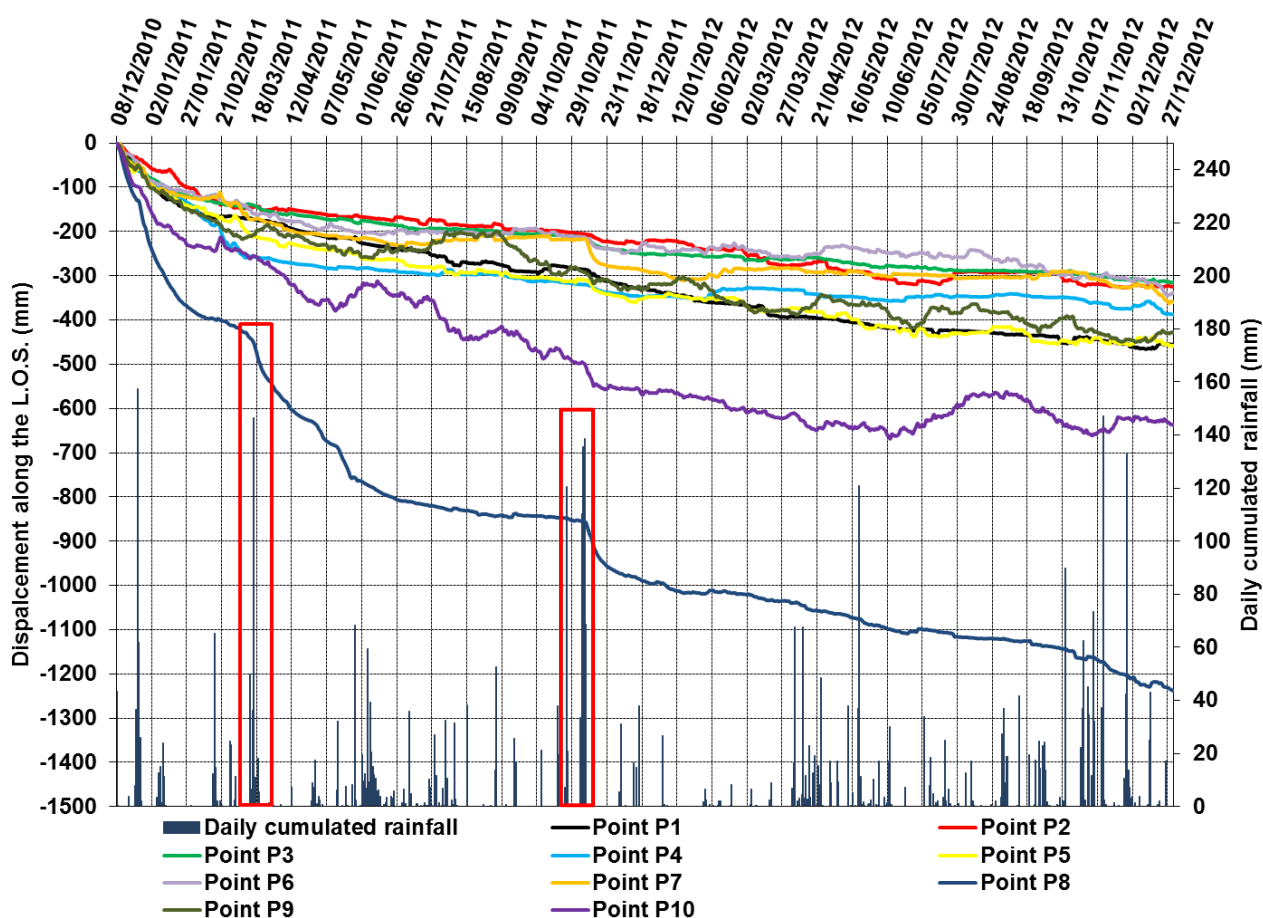


Figure 7. ICD maps of the Rotolon landslide: (a) December 8th 2010 - January 1st 2011; (b) December 8th 2010 - February 1st 2011; (c) December 8th 2010 - December 1st 2011; (d) December 8th 2010 - December 31th 2012 (Point 1-10 represent the GB-InSAR measurement points in correspondence of which the displacement time series were extracted).

From the analysis of the collected GB-InSAR dataset of the ICD maps (Fig. 7) four distinct areas characterized by relevant residual cumulated displacement were identified (Fig. 7d):

- Area 1 (ICD=737 mm, about 12500 m² in extension) and Area 2 (ICD=751 mm, area of 28000 m²), corresponding to the material infilling the detachment sector (Fig. 2), such as minor rock fall and rock avalanche deposits;

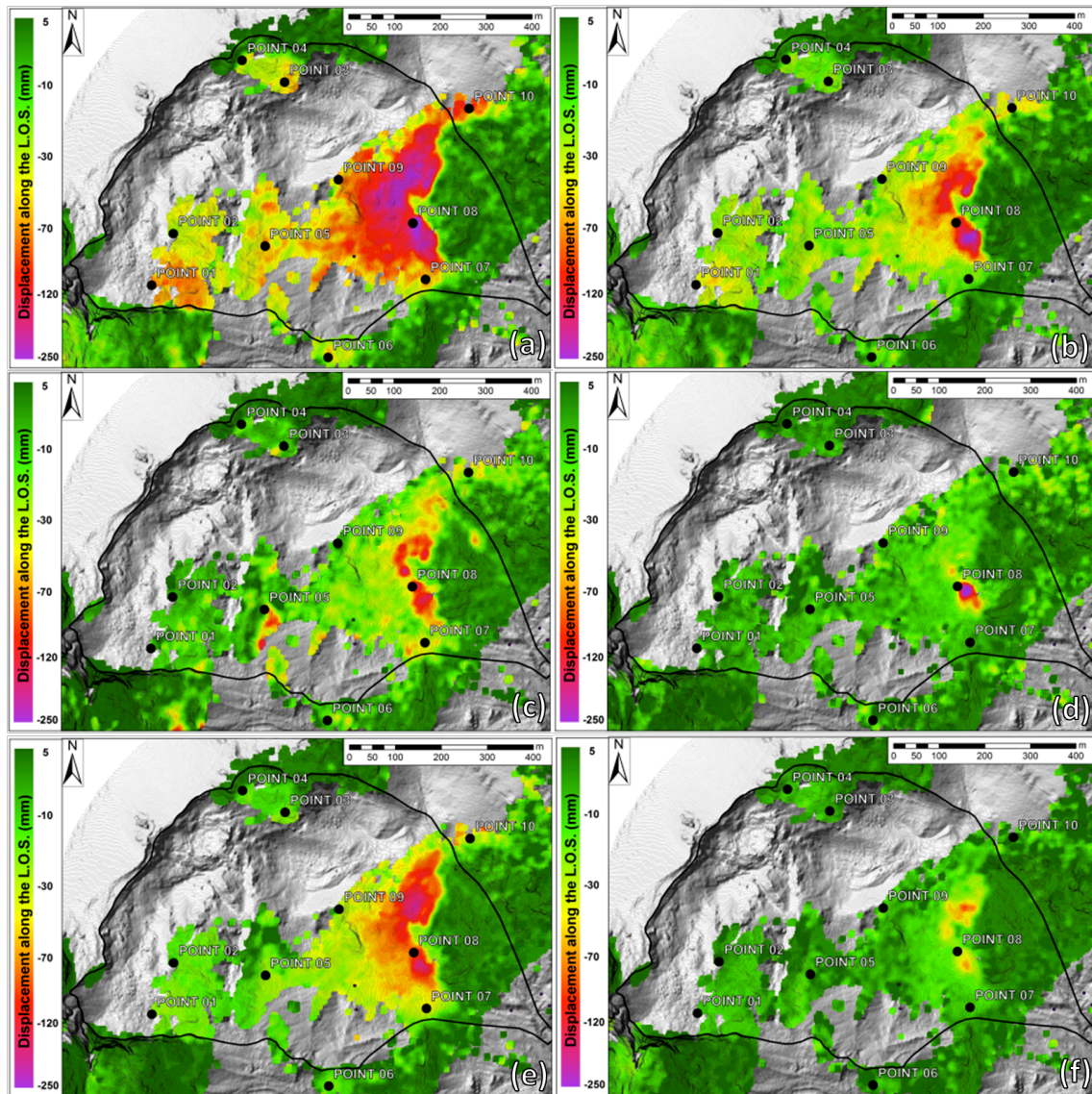
273 - Area 3 (ICD=960 mm; 12000 m² in extension) and Area 4 (ICD=2437 mm; 88000 m² coverage), both falling within
 274 the dismantling sector detrital cover (Fig. 2) which was not affected by the 2010 debris flow detachment.
 275 The measuring points time series (Fig. 8) display cumulated displacements ranging from 337 mm (Point 6) to 595 mm
 276 (Point 4, located in Area 1); Point 8 in particular (falling within Area 4) displays the monitored area cumulated peak
 277 displacements (ICD=1476 mm), showing two acceleration periods (middle March 2011 and beginning of November
 278 2011), alternating with a more linear trend. The comparison amongst the MCD maps highlighted a first phase of
 279 widespread residual displacements (December 2010, Fig. 9a), which gradually decreased from the following month
 280 (Fig. 9b). In the subsequent period ground deformation took place in correspondence with limited sectors within Area 4
 281 (May 2011 in particular shows higher MCD up to 244 mm; Fig. 9d), except for a widespread reactivation recorded in
 282 November 2011 (Fig. 9e).



283
 284 **Figure 8.** Selected measuring points displacement time series of the monitored scenario (red squares enhance Point 8
 285 accelerations).

286 Furthermore, in order to automatically extract the most hazardous residual displacement sectors, the MCD dataset was
 287 analysed by means of a MATLAB code (Salvatici et al., 2017) (Fig. 10). The code extracts from the dataset all of the
 288 areas affected by deformation higher than a selected threshold value, set equal to 92.3 mm, being the minimum
 289 displacement among all the maximum MCD values. The results are displacement maps showing only the areas with
 290 such selected displacements (Fig.10 a-d), confirming the trend highlighted by the MCD maps (Fig. 9). The second
 291 operation of the employed code consists in the frequency calculation of the displacement occurred (the code computes
 292 how many times each pixel has recorded the selected displacement during the monitoring period) (Fig. 10e). By using

293 this method, three critical areas characterized by repeated residual reactivations were detected: Area 2, Area 3 (1
 294 reactivation) and especially Area 4 (8 reactivations).
 295



296
 297 **Figure 9.** Selection of MCD maps from the GB-InSAR dataset: (a) December 2010 (232 mm cumulated peak
 298 displacement); (b) January 2011 (214 mm); (c) March 2011 (173 mm); (d) May 2011 (244 mm); (e) November 2011
 299 (174 mm); (f) November 2012 (106 mm).

300

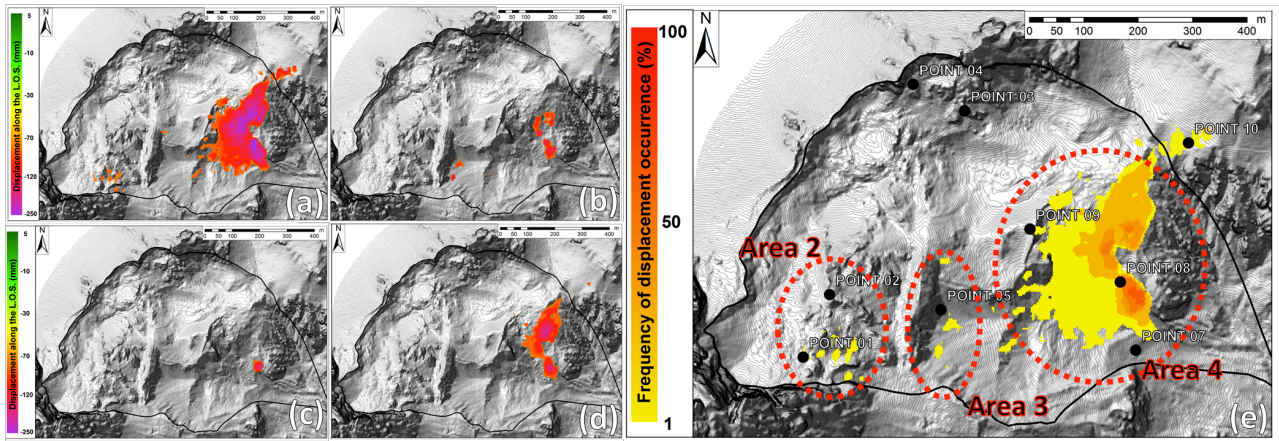


Figure 10. Residual reactivation maps obtained from selected MCD maps by means of the employed MATLAB code analysis: a) December 2010; (b) March 2011; (c) May 2011; (d) November 2011; (e) frequency map of the reactivation of the critical residual displacement sectors, classified based on their activation frequency.

6. Discussion

Successful strategies for landslide residual hazard assessment and risk reduction would imply integrated methodologies for instability detection, mapping, monitoring and forecasting (Confuorto et al., 2017). In order to provide information on the nature, extent and activation frequency of ancient landslides, standard detection and mapping procedures need a combination of field-based studies and advanced techniques, such as remote sensing data analysis and geophysical investigations (Ciampalini et al., 2015; Lotti et al., 2015; Del Soldato et al., 2016; Morelli et al., 2017; Pazzi et al., 2017a, b). In this context GB-InSAR represents a versatile and flexible technology, allowing for rapid changes in the type of data acquisition (geometry and temporal sampling) based on the characteristics of the monitored slope failure, which is capable of assessing the extent and the magnitude of the landslide residual hazard (Di Traglia et al., 2014; 2015; Carlà et al., 2016a, b). In the presented case study the 2 year continuous GB-InSAR monitoring campaign made it possible to measure the slope displacement with millimetric accuracy over a 1.2 km square landslide area, enabling the analyses of the evolution pattern connected to the landslide residual hazard. The measured deformation pattern ~~is~~was almost always consistent, in terms of extent and values, with the results obtained in some specific benchmark by an automated total station monitoring network (Frigerio et al., 2014; Bossi et al., 2015), working approximately in parallel with the GB-InSAR system. ~~(Frigerio et al., 2014; Bossi et al., 2015).~~

By comparing the landslide geomorphological map (Frodella et al., 2014) with the ICD displacement map of whole monitored period (Fig. 11), the four critical areas shown in Figure 7 are analysed in detail:

- Area 1, including measuring Points 3 and 4, is located in the northern side of detachment sector (Fig. 11a). In the first few months (between December 2010 and March 2011) the points recorded a peak of displacements of about 260 mm (Point 4) and 150 mm (Point 3); after this period the displacement decreased up to 8th November 2011. Between November 8th and 12th, during a major rainfall event (68 mm), the displacements increased again (Fig. 11b). The displacements recorded by the points within Area 1 may be related to deformations affecting the deposits placed along the steep scarp connected to the main crown delimiting the DSGSD (Fig. 4).

- Area 2 is located in the detachment sector (SW side of the DSGSD). Two measuring points (Points 1 and 2) therein located (Fig. 11d) recorded a peak of displacement of about 170 mm (Point 1) and 130 mm (Point 2) respectively, between December 2010 and March 2011. The ground deformations recorded by these points are related to slope waste

331 deposition due to the gravity affecting the coarse material infilling this sector, such as ancient rock avalanche deposits
332 (Point 1) and detensioned rock mass portions (Point 2) (Fig. 4).

333 - Area 3 represents the border between detachment and dismantling sectors, and is located upstream of the 2010 event
334 scarp (Fig.11c). Its kinematics is represented by Point 5 behavior, showing a trend similar to P1, which may be
335 associated with the sliding of the partly cemented and stabilized detrital cover material (Figs. 4-11d).

336 - Area 4 represents the lowermost portion of dismantling sector. Three measuring points are therein located: Points 7, 8
337 and 9 (Figs. 11e and 11f). Points 7 and 8 display the kinematics the detrital cover surrounding the 2010 debris flow
338 triggering area. Both control points show acceleration periods alternating with- periods of stability. In particular, the
339 trend of P8, located near the Rotolon creek ephemeral springs and channels (Frodella et al., 2014; 2015) shows a
340 correlation with cumulative precipitation above a threshold value of about 100 mm (Fig. 11f), which contribute to the
341 sub-surface water circulation within the detachment sector's loose detrital cover.

342 This suggests that the recorded displacements may be associated to the spring erosion within the detrital cover. This
343 point records the maximum displacement of the entire area (about ICD=1236 mm) monitored by GB-InSAR system.
344 The area is apparently dominated by superficial processes, such as widespread soil erosion and slope-waste deposition
345 due to gravity. Measuring Point 9, located near the dismantling sector upstream limit, records cumulative displacement
346 of 445 mm and shows an irregular trend mainly due to its location near vegetated areas (Figs. 4-11f).

347

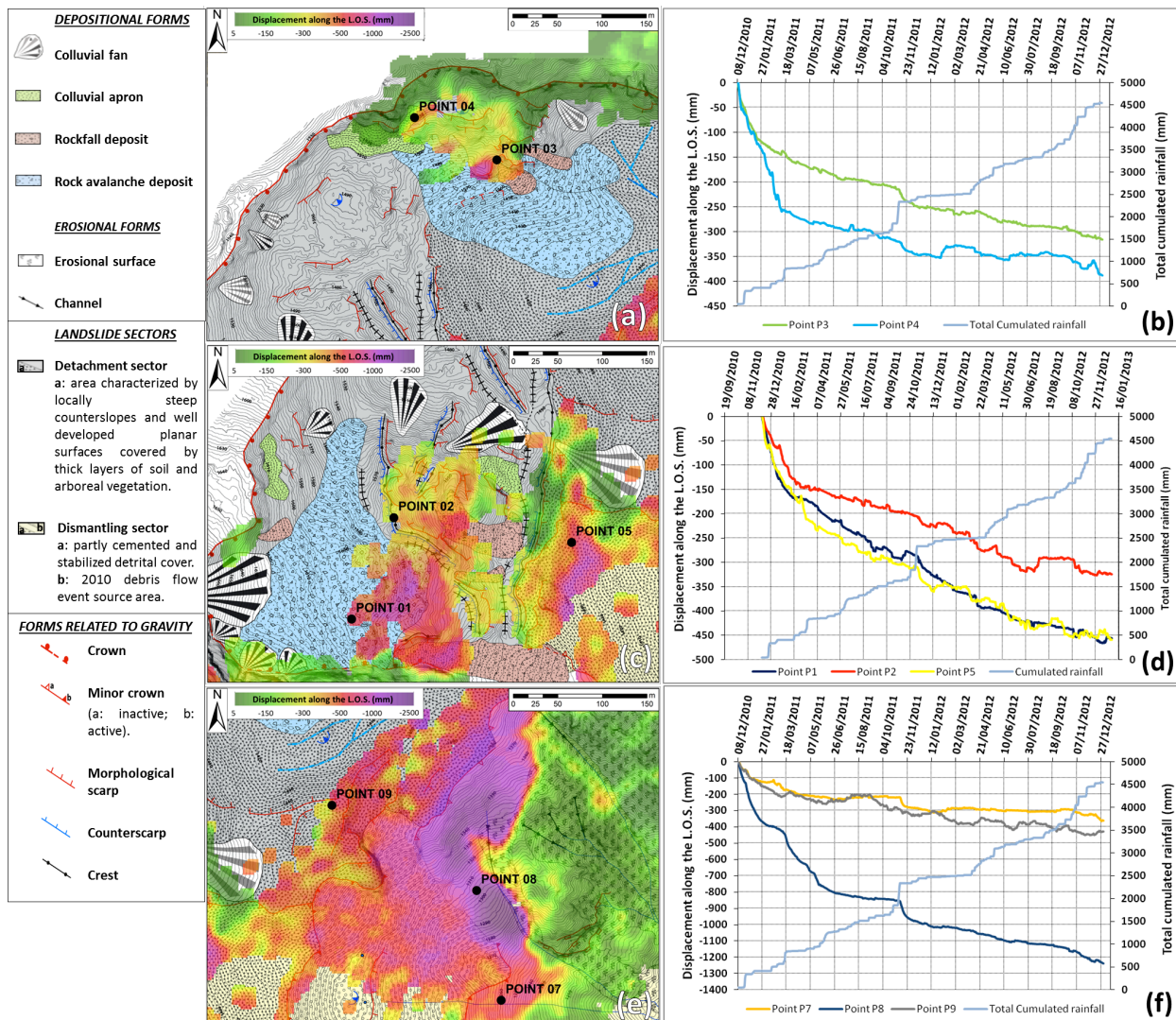


Figure 11. Integration between geomorphological map (modified after Frodella et al., 2014), the ICD maps displacement maps of whole monitored period, and the control points displacements time series: (a) the zoom of the Area 1 shown in Figure 7d; (b) the displacements time series of P4 and P3; (c) zoom of the Area 2 and Area 3 shown in Figure 7d; (d) the displacement time series of Points 1, 2 and 5; (e) zoom of Area 4 shown in Figure 7d; (f) the displacement time series of Points 7, 8 and 9.

The use of GB-InSAR ICD maps and the integration with geomorphological field surveys proved its usefulness in recognizing Area 4 (located within the DSGSD dismantling sector; Figs. 3 and 7) as the most hazardous sector within the monitored scenario, due to the widespread and intense recorded cumulated displacements (2437 mm), and its geomorphological features (steep slope, loose very coarse debris and widespread surface erosional processes in act due to the presence of ephemeral springs), and frequency of reactivations (Fig. 10).

The main triggering factor for these shallow remobilizations ongoing in this area is intense rainfall events, as highlighted by measuring point 8 time series (Fig. 8). Area 3 (recording 960 mm of total cumulated displacements) falls as well within the **Dismantling-dismantling** sector detrital cover, and was considered the second most hazardous landslide sector within the monitored scenario. Other areas characterized by relevant residual cumulated displacement were identified in Area 1 (737 mm) and Area 2 (751 mm), corresponding to the material infilling the **Detachment detachment** sector (Fig. 2), but they were not considered hazardous due to a 300 meter long and 20 meter high N-S

trending trench acting as a physical barrier separating the upper detachment sector from the lowermost dismantling sector. Furthermore, the comparison amongst the MCD maps (Fig. 9 and 10) highlighted widespread and frequent residual displacements taking place in Area 4 during the wet autumn-winter months (December 2010=232 mm; January 2011=214 mm; March 2011=173 mm; November 2011, 2012=174 and 106 mm respectively). Nevertheless, in May 2011 Area 4 reached the highest MCD in the monitored period (244 mm), although concentrated in a limited sector located near the measuring Point 8 (Fig. 9d).

~~A simplified local scale early warning system (Intrieri et al., 2012) was implemented based on three different warning levels: ordinary, pre alarm and alarm levels (Figure 5). In order to ensure the safety of the post recovery management personnel, hourly displacement thresholds were adopted: the level change occurred if the following thresholds were surpassed (i) ordinary: <1 mm/h; ii) pre alarm: 1.0 mm/h to 5.0 mm/h; iii) alarm level: >5 mm/h). Communication, which is a fundamental issue of every early warning system (Intrieri et al. 2013), was operated through the dispatch of monitoring bulletins every week and whenever the warning thresholds were exceeded.~~ In this framework, based on the surface of the deformation areas and the increasing trends of displacement time series, 4 ~~monitoring alerts~~ messages were obtained and communicated: i) March 19th 2011 (pre-alarm condition); ii) April 7th 2011 (alarm condition); iii) 8-12th November 2011 (pre-alarm condition); iv) November 10-12th 2012 (pre-alarm condition, (Fig. 6). All these events were located in the area monitored by measuring Point 8, but under none of these circumstances, the debris developed in-. ~~Inspections carried out by the optical monitoring device and by means of field surveys from safe viewing points, assessed that the detected accelerations did not generate significant slope failures and runout,~~ although rainfall comparable to that of November 2010 had hit the area every time. ~~Following the second alert, a weekly bulletin phase (May 2011 – September 2012) was planned for a residual risk prevention strategy. In any case, the GB-InSAR, benefiting from extensive coverage of the observations, registered in details a brief dislocation of surficial material and followed the gradual return to the stability conditions up to the most critical observed pixels that from time to time appeared irregularly dislocated around point 8.~~

7. Conclusions

In the context of the 2010 hazardous events affecting the Rotolon creek valley, a local scale GB-InSAR system was implemented for: i) mapping and monitoring slope landslide residual deformations; ii) early warning purposes in case of landslide reactivations. The objective was to assure the safety of both the valley's inhabitants and the personnel involved in the post-event recovery phase. The radar system acquired GB-InSAR data every 10 minutes, from which cumulated 2D displacement maps, and displacements time series of 10 measuring points were obtained. The analysed GB-InSAR data were uploaded both on a dedicated Web-based interface and remote ftp server, allowing for: i) a daily near real time and on-routine data visualization; ii) on demand analysis in case of critical weather events. In this context, based on the surface of the deformation areas and the increasing trends of displacement time series, 4 monitoring alerts were obtained and a 16 month weekly monitoring bulletin campaign was performed (May 2011-September 2012). All of the monitoring data were shared with the technical stakeholders and decision makers involved in the emergency management.

Given the recorded residual deformations, four critical sectors were identified in the monitored scenario on the basis of the measured cumulated displacements, frequency of activation and geomorphological features. Amongst these sectors Area 3 and in particular Area 4 (recording respectively 960 mm and 2437 mm of total cumulated displacements) were considered the most hazardous for potential debris flow reactivations. The latter areas are in fact located within a steep landslide sector characterized by loose detrital cover, affected by soil erosion and slope-waste deposition (~~Dismantling~~

dismantling sector). The displacement time series of the GB-InSAR measuring points provided information on the landslide kinematics: displacements range from 337 mm (Point 6) to 1476 mm (Point 8). This latter point displays the monitored area's cumulated peak displacements, showing two acceleration periods (mid March 2011 and beginning of November 2011) triggered by intense precipitations, alternating with a more linear trend. The kinematics of the other representative measuring points, is related either to deformations affecting the deposits placed along the steep scarp connected to the main DSGSD (Points 3-4), or to slope waste deposition due to gravity affecting the coarse material infilling the ~~Detachment~~ detachment sector (Points 1-2-5).

The comparison amongst the MCD maps highlighted a first phase of widespread residual displacements (December 2010). In the following period, ground deformation took place in limited sectors within Area 4, except for a widespread reactivation recorded in November 2011. The acquired radar data suggest a complex nature of the monitored landslide: its geomorphological features (e.g., rough topography, stepped profile in its upper sector, showing scarps, counterscarps, ridges, trenches and counter slopes, toe bulging) documents the activity of deep-seated long-term processes. The radar data also recorded the wide spectrum of short-term secondary instability phenomena, probably related to erosional-depositional gravitational processes (detachment sector), and soil erosion/slope-waste deposition (dismantling sector). Although this latter sector represents the most hazardous area within the landslide, the displacements acting therein during the analysed time span, appear to be related to ephemeral spring erosion located within the loose detrital cover. This suggests that these processes are only the surficial and secondary expression of a more complex deep-seated landslide system.

The monitoring system adopted provided all of the technical personnel and decision-making local authorities involved in the post-crisis management activities with a reliable, rapid and easy communication system of the results of the monitoring campaign. This favoured an enhanced understanding of such a critical landslide scenario (a populated mountainous area particularly devoted to touristic activities), during the post-emergency management activities. Furthermore, the methodology could be profitably adapted, modified, and updated in other geological contexts.

Acknowledgements

The GB-InSAR apparatus used in this application was designed and produced by Ellegi s.r.l., and based on the proprietary LiSALAB GB-InSAR technology, derived from the evolution and improvement of LiSA technology (licensed by the Ispra Joint Research Centre of the European Commission). We also would like to thank the Veneto Soil Defence Regional Direction for providing Lidar and aerial photo data.

References

- Abellán, A., Vilaplana, J.M. and Martínez, J.: Application of a long-range terrestrial laser scanner to a detailed rockfall study at Vall de Núria (Eastern pyrenees, Spain), Eng. Geol., 88, 136–148, 2006.
- Agliardi, F., Crosta, G. and Zanchi A.: Structural constraints on deep-seated slope deformation kinematics. Eng. Geol., 59, 1-2, 83-102, 2001.
- Antonello, G., Casagli, N., Farina, P., Leva, D., Nico, G., Sieber, A.J. and Tarchi D.: Ground-based SAR interferometry for monitoring mass movements, Landslides, 1, 21–28, 2004.
- Bamler, R. and Hartl, P.: Synthetic aperture radar interferometry, Inverse Probl., 14, 1–54, 1998.
- Bardi, F., Frodella, W., Ciampalini, A., Bianchini, S., Del Ventisette, C., Gigli, G., Fanti, R., Moretti, S., Basile, G. and Casagli, N.: Integration between ground based and satellite SAR data in landslide mapping: the San Fratello case study, Geomorphology, 223, 45-60, 2014.

447 Bardi, F., Raspini, F., Frodella, W., Lombardi, L., Nocentini, M., Gigli, G., Morelli, S., Corsini, A. and Casagli, N.:
 448 Monitoring the Rapid-Moving Reactivation of Earth Flows by Means of GB-InSAR: The April 2013 Capriglio
 449 Landslide (Northern Appennines, Italy), *Remote Sensing*, 9(2), 165, 2017a.

450 Bardi, F., Raspini, F., Frodella, W., Lombardi, L., Nocentini, M., Gigli, G., Morelli, S., Corsini, A. and Casagli, N.:
 451 Remote sensing mapping and monitoring of the Capriglio landslide (Parma Province, northern Italy). In Mikos, M.,
 452 Arbanas, Ž., Yin, Y., Sassa, K. (Eds) *Advancing culture of living with landslides, Vol 3 - Advances in Landslide*
 453 *Technology*, Springer International Publishing, Switzerland, pp 231-238, 2017b. Doi: 10.1007/978-3-319-53487-9_26.

454 Bertolaso, G., De Bernardinis, B., Bosi, V., Cardaci, C., Ciolli, S., Colozza, R., Cristiani, C., Mangione, D., Ricciardi,
 455 A., Rosi, M., Scalzo, A. and Soddu P.: Civil protection preparedness and response to the 2007 eruptive crisis of
 456 Stromboli volcano, Italy, *Journal of Volcanology and Geothermal Research*, 182, 269–277, 2009.

457 Bossi, G., Crema, S., Frigerio, S., Mantovani, M., Marcato, G., Pasuto A., Schenato L. and Cavalli M.: The Rotolon
 458 catchment early-warning system. In: Lollino G et al. (eds.), *Engineering Geology for Society and Territory*. Springer
 459 International Publishing 3: 91-95, 2015. DOI: 10.1007/978-3-319- 09054-2_18.

460 Broussolle, J., Kyovtorov, V., Basso, M., Ferraro Di Silvi, E., Castiglione, G., Figueiredo Morgado, J., Giuliani, R.,
 461 Oliveri, F., Sammartino, P.F. and Tarchi, D.: MELISSA, a new class of ground based InSAR system. An example of
 462 application in support to the Costa Concordia, *ISPRS J. Photogramm. Remote Sens.*, 91, 50–58, 2014.

463 Carlà, T., Intrieri, E., Di Traglia, F. and Casagli, N.: A statistical-based approach for determining the intensity of unrest
 464 phases at Stromboli volcano (Southern Italy) using one-step-ahead forecasts of displacement time series, *Natural*
 465 *Hazards*, 84(1), 669-683, 2016.

466 Carlà, T., Intrieri, E., Di Traglia, F., Nolesini, T., Gigli, G. and Casagli, N.: Guidelines on the use of inverse velocity
 467 method as a tool for setting alarm thresholds and forecasting landslides and structure collapses, *Landslides*, 14, (2),
 468 517–534, 2017.

469 Casagli, N., Catani, F., Del Ventisette, C. and Luzi, G.: Monitoring, prediction, and early warning using ground-based
 470 radar interferometry. *Landslides* 7(3):291-301, 2010.

471 Casagli, N., Frodella, W., Morelli, S., Tofani, V., Ciampalini, A., Intrieri, E., Raspini, F., Rossi, G., Tanteri, L. and Lu,
 472 P.: Spaceborne, UAV and ground-based remote sensing techniques for landslide mapping, monitoring and early
 473 warning. *Geoenvironmental Disasters* 4(9) DOI 10.1186/s40677-017-0073-1, 2017a.

474 Casagli, N., Tofani, V., Morelli, S., Frodella, W., Ciampalini, A., Raspini, F., and Intrieri, E.: Remote Sensing
 475 Techniques in Landslide Mapping and Monitoring, Keynote Lecture. In Mikos, M., Arbanas, Ž., Yin, Y., Sassa, K.
 476 (Eds) *Advancing culture of living with landslides, Vol 3 – Advances in Landslide Technology*, Springer International
 477 Publishing, Switzerland, pp 1-19, 2017b. doi: 10.1007/978-3-319-53487-9_1.

478 Casu, F., Manzo, M. and Lanari, R.: A quantitative assessment of the SBAS algorithm performance for surface
 479 deformation retrieval from DInSAR data. *Remote Sensing of Environment.*, 102 (3-4), 195-210, 2006.

480 Chandler, J.: Effective application of automated digital photogrammetry for geomorphological research, *Earth Surface*
 481 *Processes and Landforms*, 24, 51–63, 1999.

482 Ciampalini, A., Raspini, F., Bianchini, S., Frodella, W., Bardi, F., Lagomarsino, D., Di Traglia, F., Moretti, S., Proietti,
 483 C., Pagliara, P., Onori, R., Corazza, A., Duro, A., Basile, G. and Casagli, N.: Remote sensing as tool for development of
 484 landslide databases: The case of the Messina Province (Italy) geodatabase, *Geomorphology*, 249, 103-118, 2015.

485 Ciampalini, A., Raspini, F., Frodella, W., Bardi, F., Bianchini, S. and Moretti, S.: The effectiveness of high-resolution
 486 LiDAR data combined with PSInSAR data. *Landslides*, 13 (2), 399-410, 2016.

487 Confuorto, P., Di Martire, D., Centolanza, G., Iglesias, R., Mallorqui, J.J., Novellino, A., Plank, S., Ramondini, M.,
 488 Thuro, K. and Calcaterra, D.: Post-failure evolution analysis of a rainfall-triggered landslide by multi-temporal
 489 interferometry SAR approaches integrated with geotechnical analysis. *Remote Sensing of Environment*, 188, 51-72,
 490 2017.

491 Crosta G.B.: Landslide, spreading, deep seated gravitational deformation: Analysis, examples, problems and proposals.
 492 *Geografia Fisica e Dinamica Quaternaria*, 19: 297–313, 1996.

493 Crosta, G.B. and Agliardi, F.: Failure forecast for large rock slides by surface displacement measurements. *Canadian*
 494 *Geotechnical Journal*, 40(1), 176–191, 2003.

495 Cruden, D.M. and Varnes, D.J.: Landslides Types and Processes. In: Turner AK, Schuster RL (eds.), *Landslides:*
 496 *Investigation and Mitigation*. Transportation Research Board Special Report 247, National Academy Press, WA, 36–75,
 497 1996.

498 Del Soldato, M., Segoni, S., De Vita, P., Pazzi, V., Tofani, V. and Moretti, S.: Thickness model of pyroclastic soils
 499 along mountain slopes of Campania (southern Italy). In: Aversa et al. (Eds.). *Landslides and Engineered Slopes.*
 500 *Experience, Theory and Practice*. Associazione Geotecnica Italiana, Rome, Italy. ISBN:978-1-138-02988-0, 2016.

501 Del Ventisette, C., Intrieri, E., Luzi, G., Casagli, N., Fanti, R. and Leva, D.: Using ground based radar interferometry
 502 during emergency: The case of the A3 motorway (Calabria Region, Italy) threatened by a landslide, *Natural Hazards*
 503 *and Earth System Science*, 11(9), 2483-2495, 2011.

504 De Zanche V. and Mietto P.: Review of the Triassic sequence of Recoaro (Italy) and related problems. *Rend. Soc. Geol.*
 505 *It., Padova*. 25-28, 1981.

506 Di Traglia, F., Intrieri, E., Nolesini, T., Bardi, F., Del Ventisette, C., Ferrigno, F., Frangioni, S., Frodella, W., Gigli, G.,
 507 Lotti, A., Tacconi Stefanelli, C., Tanteri, L., Leva, D. and Casagli N.: The ground-based InSAR monitoring system at
 508 Stromboli volcano: Linking changes in displacement rate and intensity of persistent volcanic activity, *Bulletin of*
 509 *volcanology*, 76(2), 786, 2014a.

510 Di Traglia F., Nolesini, T., Intrieri, E., Mugnai, F., Leva, D., Rosi, M. and Casagli N.: Review of ten years of volcano
 511 deformations recorded by the ground-based InSAR monitoring system at Stromboli volcano: a tool to mitigate volcano
 512 flank dynamics and intense volcanic activity, *Earth-Sci. Rev.*, 139, 317–335, 2014b.

513 Di Traglia, F., Battaglia, M., Nolesini, T., Lagomarsino, D. and Casagli N.: Shifts in the eruptive styles at Stromboli in
 514 2010–2014 revealed by ground-based InSAR data, *Scientific Reports*, 5, 13569, 2015.

515 Fidolini, F., Pazzi, V., Frodella, W., Morelli, S. and Fanti, R.: Geomorphological characterization, monitoring and
 516 modeling of the Monte Rotolon complex landslide (Recoaro terme, Italy), *Engineering Geology for Society and*
 517 *Territory*, 2, 1311-1315. Springer International Publishing, 2015.

518 Frigerio, S., Schenato, L., Bossi, G., Cavalli, M., Mantovani, M., Marcato, G. and Pasuto, A.: A web-based platform for
 519 automatic and continuous landslide monitoring: The Rotolon (Eastern Italian Alps) case study. *Computers &*
 520 *Geosciences* 63: 96-105, 2014. DOI: 10.1016/j.cageo.2013.10.015.

521 Frodella, W., Morelli, S., Fidolini, F., Pazzi, V. and Fanti R.: Geomorphology of the Rotolon landslide (Veneto region,
 522 Italy), *Journal of Maps*, 10(3), 394-401, 2014.

523 Frodella, W., Fidolini, F., Morelli, S. and Pazzi, V.: Application of Infrared Thermography for landslide mapping: the
 524 Rotolon DSGDS case study, *Rend. Online Soc. Geol. It.*, 35, 144-147, 2015.

525 Frodella, W., Ciampalini, A., Gigli, G., Lombardi, L., Raspini, F., Nocentini, M., Scardigli, C. and Casagli, N.:
 526 Synergic use of satellite and ground based remote sensing methods for monitoring the San Leo rock cliff (Northern
 527 Italy), *Geomorphology* 264:80-94, 2016.

528 Frodella, W., Morelli, S. and Pazzi, V.: Infrared Thermographic surveys for landslide mapping and characterization: the
529 Rotolon DSGSD (Norther Italy) case study, *Italian Journal of Engineering Geology and Environment*. Accepted in
530 press, 2017. DOI: 10.4408/IJEGE.2017-01.S-07.

531 Gigli, G., Frodella, W., Mugnai, F., Tapete, D., Cigna, F., Fanti, R., Intrieri, E. and Lombardi L.: Instability
532 mechanisms affecting cultural heritage sites in the Maltese Archipelago, *Nat. Hazards Earth Syst. Sci.* 12:1-2, 2012.

533 Gigli, G., Intrieri, E., Lombardi, L., Nocentini, M., Frodella, W., Balducci, M., Venanti, L.D. and Casagli, N.: Event
534 scenario analysis for the design of rockslide countermeasures, *J. Mt. Sci.*, 11(6), 1521–1530, 2014a.

535 Gigli, G., Frodella, W., Garfagnoli, F., Mugnai, F., Morelli, S., Menna, F. and Casagli, N.: 3-D geomechanical rock
536 mass characterization for the evaluation of rockslide susceptibility scenarios, *Landslides*, 11(1), 131-140, 2014b.

537 Gigli, G., Morelli, S., Fornera, S., and Casagli, N.: Terrestrial laser scanner and geomechanical surveys for the rapid
538 evaluation of rock fall susceptibility scenarios. *Landslides*, 11(1), 1-14, 2014c.

539 Gullà, G., Peduto, D., Borrelli, L., Antronico, L. and Fornaro, G.: Geometric and kinematic characterization of
540 landslides affecting urban areas: the Lungro case study (Calabria, Southern Italy). *Landslides* 14:171–188, 2017.
541 doi:10.1007/s10346-015-0676-0.

542 Guzzetti, F., Mondini, A.C., Cardinali, M., Fiorucci, M., Santangelo, M. and Chang, K.T.: Landslide inventory maps:
543 new tools for an old problem, *Earth Science Reviews*, 112, 1–25, 2012.

544 Intrieri, E., Gigli, G., Mugnai, F., Fanti, R. and Casagli, N.: Design and implementation of a landslide early warning
545 system, *Engineering Geology*, 147, 124-136, 2012.

546 Intrieri, E., Gigli, G., Casagli, N. and Nadim, F.: Brief communication" Landslide Early Warning System: toolbox and
547 general concepts", *Natural hazards and earth system sciences*, 13(1), 85-90, 2013.

548 Jaboyedoff, M., Oppikofer, T., Abellán, A., Derron, M.H., Loye, A., Metzger, R. and Pedrazzini, A.: Use of LIDAR in
549 landslide investigations: a review, *Natural hazards*, 61(1), 5-28, 2012.

550 Lombardi, L., Nocentini, M., Frodella, W., Nolesini, T., Bardi, F., Intrieri, E., Carlà, T., Solari, L., Dotta, G., Ferrigno,
551 F. and Casagli, N.: The Calatabiano landslide (southern Italy): preliminary GB-InSAR monitoring data and remote 3D
552 mapping, *Landslides*:1-12, 2017.

553 Lotti, A., Saccorotti, G., Fiaschi, A., Matassoni, L., Gigli, G., Pazzi, V. and Casagli, N.: Seismic monitoring of
554 rockslide: the Torgiovanetto quarry (Central Apennines, Italy), in: G. Lollino et al. (eds), *Engineering Geology for
555 Society and Territory – Vol.2*, Springer International Publishing, Switzerland, 1537-1540. 2015. doi: 10.1007/978-3-
556 319-09057-3_272.

557 Luzi, G., Pieraccini, M., Mecatti, D., Noferini, L., Guidi, G., Moia, F. and Atzeni, C.: Ground-based radar
558 interferometry for landslides monitoring: atmospheric and instrumental decorrelation sources on experimental data,
559 *IEEE Trans. Geosci. Remote Sens*, 42(11), 2454–2466, 2004.

560 Luzi, G.: Ground Based SAR Interferometry: a novel tool for geosciences, P. Imperatore, D. Riccio (Eds.), *Geoscience
561 and Remote Sensing. New Achievements*, InTech, 1-26, 2010.

562 Monserrat, O., Crosetto, M. and Luzi, G.: A review of ground-based SAR interferometry for deformation
563 measurement, *ISPRS Journal of Photogrammetry and Remote Sensing* 93, 40-48, 2014.

564 Morelli, S., Pazzi, V., Monroy, V. H. G., and Casagli, N.: Residual Slope Stability in Low Order Streams of Anganguero
565 Mining Area (Michoacán, Mexico) After the 2010 Debris Flows. In Mikos, M., Casagli, N., Yin, Y., Sassa, K. (Eds)
566 *Advancing culture of living with landslides*, Vol 4 – Diversity of landslide forms, Springer International Publishing,
567 Switzerland, pp 651-660, 2017. doi: 10.1007/978-3-319-53485-5_75.

568 Nicodemo G, Peduto D, Ferlisi S and Maccabiani J.: Investigating building settlements via very high resolution SAR
569 sensors. In: Bakker J, Frangopol D.M., van Breugel K (eds) © 2017Life-cycle of engineering systems: emphasis on
570 sustainable Civil Infrastructure. Taylor & Francis Group, London, pp 2256–2263, 2016.

571 Nolesini, T., Di Traglia, F., Del Ventisette, C., Moretti, S. and Casagli, N.: Deformations and slope instability on
572 Stromboli volcano: Integration of GBInSAR data and analog modeling, *Geomorphology* 180, 242-254, 2013.

573 Nolesini T, Frodella W, Bianchini S and Casagli, N.: Detecting Slope and Urban Potential Unstable Areas by Means of
574 Multi-Platform Remote Sensing Techniques: The Volterra (Italy) Case Study, *Remote Sensing*, 8(9), 746, 2016.

575 Pagliara, P., Basile, G., Cara, P., Corazza, A., Duro, A., Manfrè, B., Onori, R., Proietti, C. and Sansone, V.: Integration
576 of earth observation and ground-based HR data in the civil protection emergency cycle: the case of the DORIS project,
577 in: Pardo-Igúzquiza E, Guardiola-Albert C, Heredia J, Moreno-Merino L, Durán JJ, Vargas-Guzmán JA (Eds.)
578 *Mathematics of Planet Earth, Lecture Notes in Earth System Sciences*. Springer, Berlin Heidelberg 263–266, 2014.

579 Pazzi, V., Tanteri, L., Bicocchi, G., Caselli, A., D'Ambrosio, M. and Fanti, R.: H/V technique for the rapid detection of
580 landslide slip surface(s): assessment of the optimized measurements spatial distribution. In Mikos, M., Tiwari, B., Yin,
581 Y., Sassa, K. (Eds) *Advancing culture of living with landslides, Vol 2 – Advances in landslide science*, Springer
582 International Publishing, Switzerland, pp 335-343, 2017a doi: 10.1007/978-3-319-53498-5_38.

583 Pazzi, V., Tanteri, L., Bicocchi, G., D'Ambrosio, M., Caselli, A. and Fanti, R.: H/V measurements as an effective tool
584 for the reliable detection of landslide slip surfaces: Case studies of Castagnola (La Spezia, Italy) and Roccalbegna
585 (Grosseto, Italy), *Physics and Chemistry of the Earth*, 98, 136-153, 2017b. doi:
586 <http://dx.doi.org/10.1016/j.pce.2016.10.014>.

587 Peduto D., Ferlisi S., Nicodemo G., Reale D., Pisciotta G. and Gullà G.: Empirical fragility and vulnerability curves for
588 buildings exposed to slow-moving landslides at medium and large scales, *Landslides*, in press, 2017a. doi:
589 10.1007/s10346-017-0826-7.

590 Peduto, D., Nicodemo, G., Maccabiani, J. and Ferlisi, S.: Multi-scale analysis of settlement induced building damage
591 using damage surveys and DInSAR data: a case study in The Netherlands. *Engineering Geology*, 218:117–133, 2017b.
592 doi:10.1016/j.enggeo.2016.12.018.

593 Pieraccini, M., Tarchi, D., Rudolf, H., Leva, D., Luzi, G., Bartoli, G. and Atzeni, C.: Structural static testing by
594 interferometric synthetic radar, *NDT and E Intl.*, 33(8), 565–570, 2000.

595 Pieraccini, M., Casagli, N., Luzi, G., Tarchi, D., Mecatti, D., Noferini, L. and Atzeni, C.: Landslide monitoring by
596 ground-based radar interferometry: a field test in Valdarno (Italy), *Int J Remote Sens* 24:1385–1391, 2002.

597 Salvatici, T., Morelli, S., Pazzi, V., Frodella, W. and Fanti, R.: Debris flow hazard assessment by means of numerical
598 simulations: implications for the Rotolon Creek Valley (Northern Italy), *Journal of Mountain Science*, 14 (4), 636-648,
599 2017. doi:10.1007/s11629-016-4197-7.

600 Tarchi, D., Ohlmer, E. and Sieber, A.J.: Monitoring of structural changes by radar interferometry, *Res. Nondestruct.*
601 *Eval.* 9, 213–225, 1997.

602 Tarchi, D., Casagli, N., Fanti, R., Leva, D., Luzi, G., Pasuto, A., Pieraccini, M. and Silvano, S.: Landslide monitoring
603 by using ground-based SAR interferometry: an example of application to the Tessina landslide in Italy, *Engineering*
604 *Geology*, 68, 15-30, 2003.

605 Tapete, D., Gigli, G., Mugnai, F., Vannocci, P., Pecchioni, E., Morelli, S., Fanti R., and Casagli, N.: Correlation
606 between erosion patterns and rockfall hazard susceptibility in hilltop fortifications by terrestrial laser scanning and
607 diagnostic investigations. In: *IEEE International Geoscience and Remote Sensing Symposium. Remote Sensing for a*
608 *Dynamic Earth*. Munich, Germany, 22-27 July 2012, pp. 4809-4812, 2012. ISBN 978-1-4673-1159-5.

609 Tofani, V., Raspini, F., Catani, F. and Casagli, N.: Persistent scatterer interferometry (PSI) technique for landslide
 610 characterization and monitoring. In: Sassa, K., Canuti, P., Yueping, Y. (Eds.), *Landslide Science for a Safer*
 611 *Geoenvironment Methods of Landslide Studies 2*. Springer International Publishing, pp. 351–357, 2014. ISBN:
 612 9783319050492.
 613 Zischinsky, U.: *Über sackungen*, *Rock Mech.*, 1(1), 30–52, 1969.
 614 Zhang, Z., Zheng, S. and Zhan, Z.: Digital terrestrial photogrammetry with photo total station, *International Archives of*
 615 *Photogrammetry and Remote Sensing*, Istanbul, Turkey, 232-236, 2004.